B-051 Spatio-temporal Variability and Climate Effect of Ozone and Black Carbon in Asia (Abstract of the Final Report)

Contact person Hajime Akimoto
Director, Atmospheric Composition Research Program
Frontier Research Center for Global Change
Japan Agency for Marine-Earth Science and Technology
3173-25 Showa-machi, Kanazawa-ku, Yokohama
Tel:+81-45-778-5710 Fax:+81-45-778-5496
E-mail: akimoto@jamstec.go.jp

Total Budget for FY2005-FY2007 192,070,000Yen (**FY2007**; 62,785,000Yen)

Key Words Tropospheric ozone, Black carbon, Climate effect, Observation, Chemical Transport Modeling

[Abstract]

Whole-year's observation of tropospheric ozone and black carbon (BC) has been made in the continental East to Central Asia, a blank area of measurement. Surface ozone concentration at mountain sites in the North China Plain has peaks in May-June and September whereas it maximizes in summer in Central Asia. Annual mean concentrations of black carbon are 2.3 and 1.0 $\mu g/m^3$ at Mt. Tai and Mt. Huang,, respectively, and as low as 0.10 $\mu g/m^3$ at a Kyrgyz mountain site. Intensive field campaign were made at Mt. Tai, midst of the North China Plain and Mt. Mang, the north of Beijing in June and September, respectively. Agricultural waist burning of winter wheat was found to be one of the main reason of severe air pollution in June in the North China Plain. A MAX-DOAS spectrometer and retrieval software have been developed and operated at Mt. Tai during the campaign to validate satellite data of NO_2 tropospheric column. The satellite data of OMI was found to have 20% positive bias.

Emission inventories of NOx, NMVOC, SO_2, CO, BC and OC in Asia has been completed for 1980-2020, and publicized on web page as REAS version 1.1. The future projection data was used to predict the ozone pollution in East Asia in 2020. According to the PFC scenario for China, three month average (June-August) ozone concentration in the North China Plain increases ca. 18 ppb whereas it increases ca. 6 ppb in the central part of Japan in spite of the expected decrease of NOx emission in Japan.

Climate sensitivity runs of tropospheric ozone and black carbon have been conducted using a chemical-climate model, CHASER and CCSR/NIES/FRCGC GCM. The temperature sensitivities for the concentration change of ozone and black carbon are +0.3°C and +0.5°C for global average during 1850-2000. Temperature rise due to black carbon was found to be as high as more than 1.0°C in North America, Europe and central Asian continent.

1. Introduction

Although the long-lived greenhouse gases targeted by the Kyoto Protocol have been predominantly focused so far in scientific studies related to global warming, IPCC has recently also pointed out the importance of regional climate effect of short-lived radiatively active species such as aerosols and tropospheric ozone. Nevertheless, studies related to impacts on global warming by short-lived species have long been delayed compared to long-lived greenhouse gases. Among the short-lived species tropospheric ozone and black carbon (BC) have the largest warming effect so that elucidation of their spatial distribution and temporal variability and evaluation of their regional climate effect in Asia is urgently needed from the point of more reliable prediction of future climate change in this region.

In the present study, spatial and temporal variability of ozone and aerosols in Asia are elucidated by means of ground-based observation and satellite data analysis in the region covering Central Asia to East Asia. Further, mid-term future prediction of spatio-temporal variability of these species in Asia will be made through emission inventories of precursors of ozone and aerosols, and primary aerosol, black carbon, during 2000-2020. Based on these studies, regional climate sensitivity of these species will be evaluated by chemical climate model comparing with those by long-lived greenhouse gases.

2. Research Objective

Continuous observation using automatic instruments and intensive field campaign will be made in order to evaluate inter- and intra-continental transport, photochemical budget of ozone, and emission ratios of BC/OC/CO/NOx/VOC in the regionally polluted inner land of Asian continent. Particularly, it is aimed to reduce uncertainty of emission inventories of BC and to elucidate spatial and temporal variability of ozone and aerosols in Asia. For this purpose, tropospheric chemistry satellite sensors launched in Europe and USA will also be utilized to analyze the distribution of ozone and NOx in East Asia, and the ground-based continuous MAX-DOAS observation for tropospheric NO_2 column will be made for the validation of the satellite data.

Emission inventories of precursors of ozone and aerosols as well as BC from 1995 to 2020 in Asia including Asian part of Russia and Central Asia will be made to provide input data for regional and global chemical transport/climate models in order to get more reliable spatial and temporal change, and radiative forcing. Contribution of stratospheric intrusion, inter-continental transport form Europe and North America, intra-continental transport from East, Southeast and South Asia to our country are evaluated in the view of hemispherical air pollution. Future prediction of ozone and aerosols will also be made for 2020.

One of the final goals of this study is to evaluate climate sensitivity of tropospheric ozone and black carbon for temperature field by use of chemical climate model to improve accuracy of climate change prediction.

3. Results and Discussion

(1) Ground-based observation of ozone and black carbon in Asia

We conducted continuous monitoring of tropopspheric ozone, carbon monoxide (CO), and blackcarbon (BC) at several mountainous sites in East and Central Asia region, where the observational data have not been reported before. Our observational results uncovered their general features (concentration levels, seasonal and diurnal variations) for the first time; the ozone concentrations in China have maximum in June and minimum in July/August, ozone in east Siberia has a spring peak, and ozone in Central Asia has a summer peak. Ozone concentrations observed at three mountainous sites in China increased in the air mass whose residence time over the Central East Asia region was long, suggesting the photochemical buildup in the polluted region. The BC concentrations (as measured by Multi-Angle Absorption Photometer instruments) showed autumn maxima at Taishan and Huanshan in China, with annual average concentrations being 2.3 and 1.0 micro gC/m^3, respectively. The radiative forcing at the top of atmosphere owing to the increased concentrations of BC at the present day in comparison to pre-industrial time over the Central East Asia region was as high as 1.6 W m^{-2} (Table 1), being comparable to that owing to the increased CO_2 in the atmosphere. At a mountain station in Kyrgyz, the average BC level was only 0.10 micro gC/m^3. The representativeness of the locations over the regions enables test of the chemical transport model using these observational data.

In June 2006, we performed an intensive field campaign at Mt. Tai station (1534 m asl), located in the middle of the Central East China, to reveal 1) the transportation and photochemical budget of tropospheric ozone, and 2) the concentration levels of BC, OC (organic carbon), CO, NOx, and VOC (volatile organic compounds) and their ratios over the region for the first time. The observational results of selected species are shown in Fig. 1 By comparing BC concentrations derived from four different instruments, we concluded that the uncertainty in the BC determination was less than 50%, enabling to better confine the uncertainty in the BC emission rate in China (a factor of 4). We also found that 1) open biomass burning of crop residues (winter wheat) after its harvest in early June resulted in elevated concentrations of atmospheric pollutants, 2) in-situ photochemistry was active, producing ~60 ppbv of ozone in a day under the NOx-limited conditions, 3) the emission inventory of BC and ozone precursors in China need to be increased for the model simulations to reproduce the observed levels of these

Table 1. Estimated radiative forcing at the top of atmosphere (TOA) in a global scale and over Central East China induced by selected chemical species

species	sensitivity	global			Central East China		
		Concentration (present)	Concentration (pre-industrial)	TOA radiative forcing (W m^{-2})	Concentration (present)	Concentration (pre-industrial)	TOA radiative forcing (W m^{-2})
CO_2	0.01677 W m^{-2} ppm^{-1}	379 ppm	280 ppm	1.66	390 ppm	280 ppm	1.84
CH_4	0.00045 W m^{-2} ppb-1	1774 ppb	715 ppb	0.48	1900 ppb	715 ppb	0.54
O_3	0.032 DU^{-1}	40 DU	30 DU	0.32	50 DU	30 DU	0.64
BC	1.25 W mg^{-1}	0.4 mg m^{-2}	0.2 mg m^{-2}	0.25	1.5 mg m^{-2}	0.2 mg m^{-2}	1.63

Present and pre-industrial concentrations of CH_4 and O_3 were only roughly estimated.

species, and that 4) photochemically aged air masses were observed at Mt. Tai from the analysis of NOx, NOy, VOC, and OVOC (oxygenated volatile organic compounds) levels. Our VOC measurements during the campaign were compared to those made by Institute of Atmospheric Physics, Chinese Academy of Sciences.

In Septemer/October 2007, another intensive field campaign was held in Mangshan Park, ~40 km north of the city center of Beijing, with a focus on chemical and optical properties of aerosols. There we performed an instrument comparison for BC measurements again and confirmed the relationship obtained at Mt. Tai. It is concluded that ammonium sulfate, organics, and ammonium nitrate are major chemical components of the aerosol particles, controlling scattering of the ambient aerosols and thus the visibility.

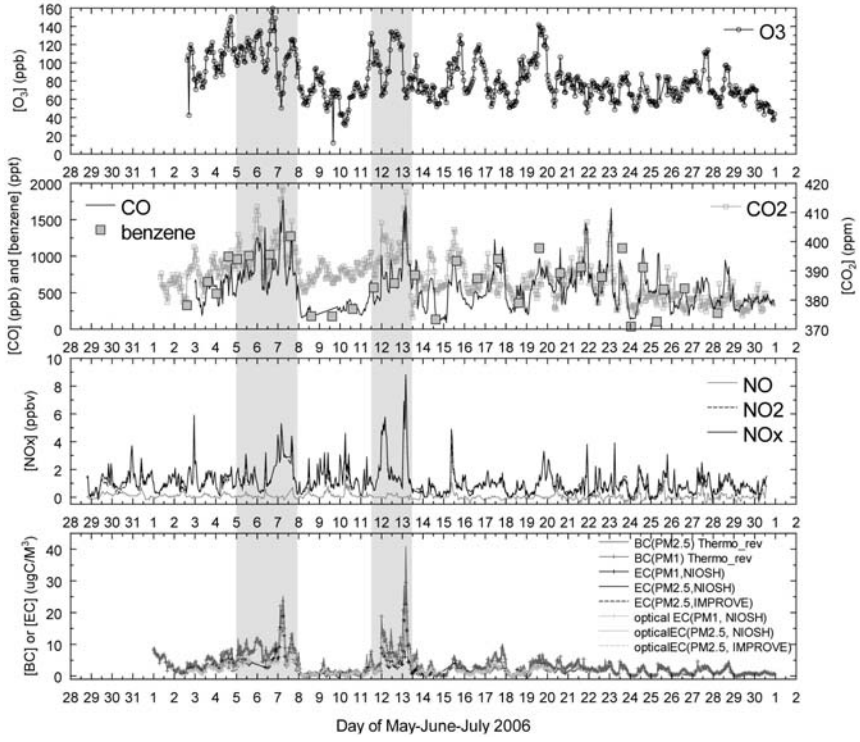

Fig. 1. Temporal variations in the observed O_3, CO, benzene, CO_2, NOx, and BC concentrations during the Mt. Tai intensive campaign.

(2) Analysis of tropospheric chemistry satellite data in Asia

Since 1995, satellite observations have provided the tropospheric column data of nitrogen dioxide (NO_2) on a global scale. The satellite observations have been shown to be crucial, for instance, to the estimate of recent trends in tropospheric NO_2 over several important regions, including polluted regions in East Asia, and to the systematic evaluation of global atmospheric chemistry models. However, although the quantitative basis for analyzing satellite data should be provided by comparisons with other independent measurements, very limited satellite-independent measurements are available in urban sites in East Asia. In FY2005, we developed a ground-based MAX-DOAS system suitable for validating satellite data. In

FY2006, we performed MAX-DOAS measurements at two sites (foot and top of Mt. Taishan) in China (Tai'an: 36.2ºN, 117.1ºE, 126 m asl, and Taishan: 36.3ºN, 117.1ºE, 1534 m asl) for about one month from May 29 to June 29, 2006. The measurements were made as part of our intensive field measurement campaign (the Taishan campaign) conducted in this project. Comparisons between tropospheric NO_2 columns measured by MAX-DOAS and OMI (the newest satellite-borne instrument measuring tropospheric gaseous pollutants) showed that OMI data have a positive bias of about 20% with a random difference as small as 8% (Fig. 2, left), suggesting that the spatial distribution of NO_2 seen by OMI (Fig. 2, right) is reliable. On the other hand, a long-term dataset of tropospheric NO_2 columns from a satellite instrument (GOME) was analyzed. Seasonal and year-to-year variations of tropospheric NO_2 columns seen by GOME were qualitatively reproduced by a regional model. We also compared tropospheric ozone columns derived from GOME with ozonesonde and other satellite data and showed that GOME data have a positive bias of about 10% and a random error of about 15-30%. Analysis of ozonesonde data showed that tropospheric ozone columns over Japan increased from 1970 to 2002 but after 2003 the increasing rate tended to be slower. These results provide the quantitative basis for interpreting the satellite/model comparison and for identifying potential problems in the models.

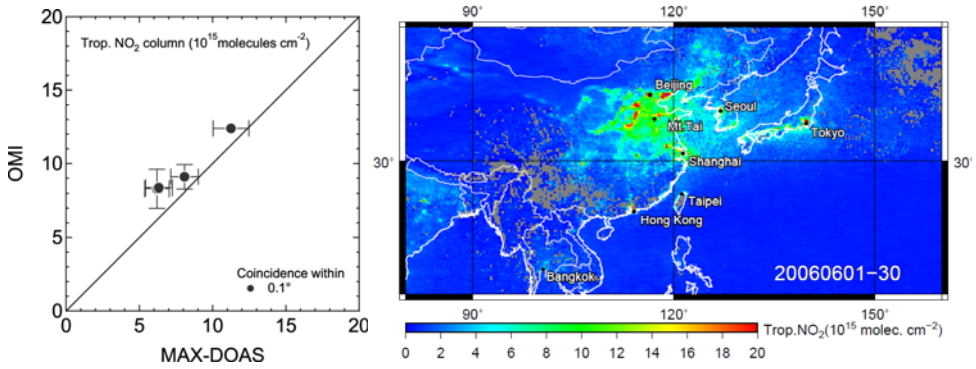

Fig. 2. (Left) Correlations between tropospheric NO_2 columns measured by OMI and MAX-DOAS in the North China Plain. (Right) Monthly-mean map of the tropospheric NO_2 column concentration measured by the satellite instrument OMI.

(3) Development of Asian emission inventory and future projection

We developed a new emission inventory for Asia (Regional Emission inventory in ASia (REAS) Version 1.1) for the period 1980–2020. REAS is the first inventory to integrate historical, present, and future emissions in Asia on the basis of a consistent methodology. We present here emissions in 2000, historical emissions for 1980–2003, and projected emissions for 2010 and 2020 of SO_2, NOx, CO, NMVOC, black carbon (BC), and organic carbon (OC) from fuel combustion and industrial sources. Total energy consumption in Asia more than doubled between 1980 and 2003, causing a rapid growth in Asian emissions, by 28% for BC, 30% for OC, 64% for CO, 108% for NMVOC, 119% for SO_2, and 176% for NOx. In particular, Chinese NOx emissions showed a marked increase of 280% over 1980 levels, and growth in emissions

since 2000 has been extremely high. These increases in China were mainly caused by increases in coal combustion in the power plant and industrial sectors. NMVOC emissions also rapidly increased because of growth in the use of automobiles, solvents, and paints. By contrast, BC, OC, and CO emissions in China showed decreasing trends from 1996 to 2000 because of a reduction in the use of biofuels and coal in the domestic and industry sectors. However, since 2000, Chinese emissions of these species have begun to increase. Thus, the emissions of air pollutants in Asian countries (especially China) showed large temporal variations from 1980–2003. Future emissions in 2010 and 2020 in Asian countries were projected by emission scenarios and from emissions in 2000. For China, we developed three emission scenarios: PSC (policy success case), REF (reference case), and PFC (policy failure case). In the 2020 REF scenario, Asian total emissions of SO_2, NOx, and NMVOC were projected to increase substantially by 22%, 44%, and 99%, respectively, over 2000 levels. The 2020 REF scenario showed a modest increase in CO (12%), a lesser increase in BC (1%), and a slight decrease in OC (–5%) compared with 2000 levels. However, it should be noted that Asian total emissions are strongly influenced by the emission scenarios for China. Additionally, the emissions for Asian region of Former Soviet Union were estimated during 1980-2005 (Fig. 3).

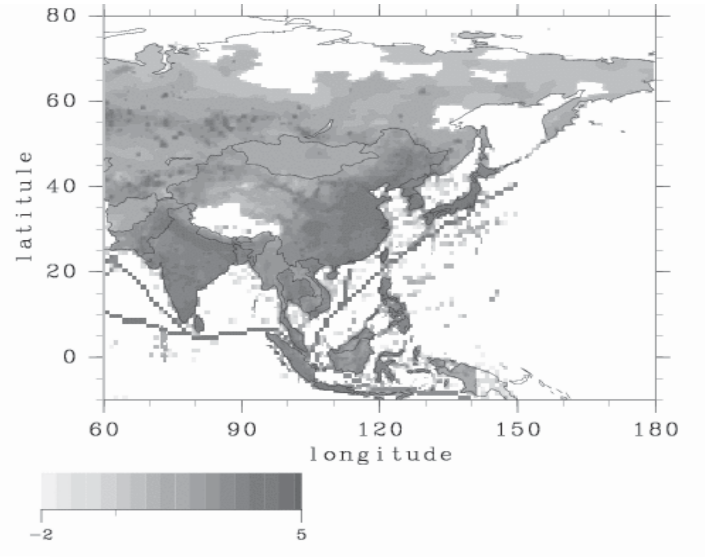

Fig. 3. Spatial distributions of NOx emissions for 2000 over the East Eurasian continent. Unit is t yr^{-1} $mesh^{-1}$ and mesh size is 0.5 degree of lat/lon. The emissions are indicated by log scale.

(4) Hemispherical pollution of ozone and black carbon studied by chemical transport models

In order to elucidate source-recepter relationship of tropospheric ozone, "tagged method" has been developed using the global chemical transport model, CHASER, and contribution of each source region to global remote sites was evaluated. Representative remote site at Mace Head, Bermuda, and Samoa receive contribution of more then 40% from polluted region in North America, Europe, and Asia. Contribution from boundary layer in China and free troposphere in Asia was discerned at almost all area in the northern hemisphere. In June to September ozone from Asian free troposphere gives large contribution of 5-10 ppb to South Pacific via inter-hemispheric long range transport from Asia to southern hemisphere over upper troposphere. Similarly, inter-hemispherical transport from South America contributes significantly to Japan,

Northern Pacific, and United States.

Another global chemical transport model FRCGC/UCI was used for evaluating contribution from Europe, North America, China, South and Southeast Asia, Japan, and stratosphere to Tokyo Metropolitan Area by means of zeroing emission method for three months during February to April. The three month averaged contribution from each region was 3.9, 3.0, 4.4, 0.8, 9.4, 12.2 ppb, respectively. Thus, the sum of inter-continental transport from Europe and North America exceeds the contribution of China in monthly average. However, while the contributions of Europe and North America are almost constant and do not vary much day by day, the impact from China is very episodic ranging from nearly 15 ppb to less than 2 ppb so that the significance cannot be evaluated only by monthly averaged values. Particularly, for the high ozone day over 80 ppb, there are different cases that either ozone from Japan predominates or ozone from Japan and China are comparable.

Using a regional chemical transport model, photochemical ozone production due to East Asian emissions of precursors has been evaluated. For Japan, contribution of photochemical ozone produced by own emission substantiates in summer, but in other season long-range transport contributes significantly to Japan. In particular its contribution predominates in winter to early spring. Future prediction of ozone pollution in East Asia in 2020 has been predicted using three scenarios for China. When the PFC scenario (business as usual) is used, three month-averaged concentration in Japan in summer (June-August) increases about 6ppb in spite of the expected decrease in NOx emission in Japan, whereas the increase is about 18 ppb in the North China Plain. Monthly averaged concentration of ozone from March to June in Japan will exceed 60ppb (one hour averaged air quality standard level).

Tagged method has also developed for a regional chemical transport model, and observation data obtained in Sub-theme 1 has been analyzed.

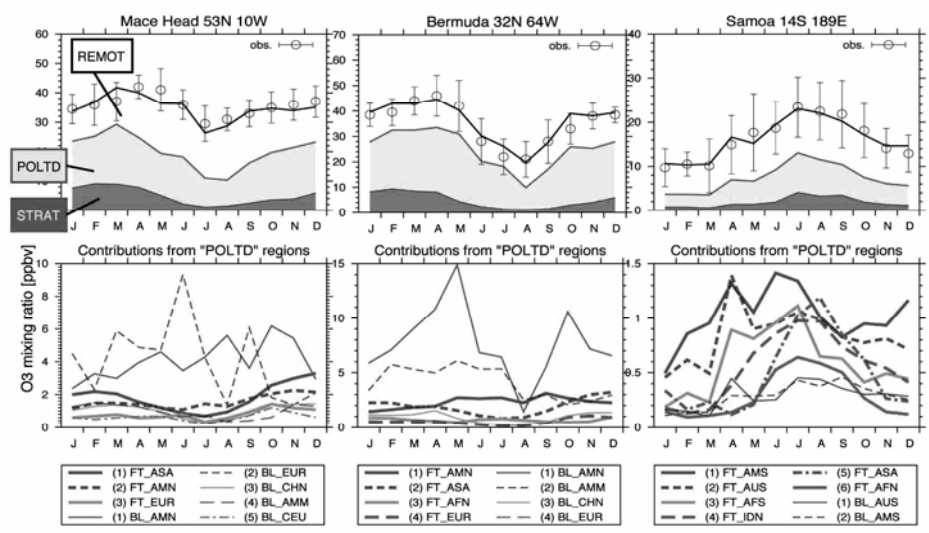

Fig. 4. Seasonal variation of contributions form different source region to the surface ozone in remote sites (Mace Head, Bermuda, Samoa)

(5) Evaluation of climate effect of ozone and black carbon studied by a chemistry-climate model

1) Evaluation of climate response to global ozone changes

We assess climate response to global tropospheric ozone changes since preindustrial times (around the year 1850) using a chemistry coupled climate simulation. Chemistry and transport of tropospheric ozone and related species are simulated by the CHASER model which is based on the CCSR/NIES/FRCGC AGCM (Sudo et al, 2002). For climate simulation in this study, CHASER is coupled with a simplified ocean model (mixed-layer ocean model). We use the global emission inventory EDGAR/HYDE for precursor emissions in preindustrial times (1850) and present days (2000). We evaluate equilibrium responses of climate to changes of tropospheric ozone from preindustrial times to present days as well as those of long-lived GHGs (LLGHGs); in this study, LLGHGs represents CO2, CH4, N2O, and CFCs. In this study, global mean surface air temperature increases by 0.3 K as a equilibrium response to the specified tropospheric ozone increases from 1850 to 2000. This is equivalent to 14% of our estimated climate sensitivity to the LLGHGs increases in this study (2.2K)(Table.1). Our simulation shows anomalously high temperature increases (0.5-1.0K) over Middle East and US which appear to reflect the inhomogeneous distributions of radiative forcing from ozone changes. Temperature increase due to tropospheric ozone increases is more significant in the upper troposphere in the low to midlatitudes. In the stratosphere, there are large temperature decreases (cooling) of -0.5 or -1.0 K associated with reduction in long-wave radiation due to upper tropospheric ozone increases. This study also evaluates the impacts of stratospheric ozone depletion since 1970s on climate. The specified stratospheric ozone decrease in the stratosphere is calculated to cool the surface by 0.04K (Table 2). This is due to reduced long-wave absorption and decreasing O3 input to the troposphere.

Table 2. Impacts on Global Average Surface Air Temperatures ΔT（K）。

	Global	NH	SH
Trop. O3	＋0.28	＋0.31	＋0.25
Strato. O3	－0.04	－0.05	－0.04
LLGHGs*	＋2.23	＋1.78	＋2.78

*LLGHGs=CO_2 + CH_4 + N_2O + CFCs.

2) Evaluation of climate response to global BC changes

We also evaluated the impacts of changes in black carbon (BC) aerosol on climate, calculating BC radiative forcing and climate responses to the present BC distribution. The estimated BC radiative forcing was about 0.5 W m^{-2}, very close to that for tropospheric ozone increase (0.48 Wm^{-2}) in this study. Fig.5 shows similar but different latitudinal patterns of ozone and BC forcing. We found outstandingly large BC forcing (>3 W m^{-2}) around India and China, which is also reflected on Fig. 5. We calculated the global mean surface temperature response to BC as 0.5℃, comparable with that for ozone (0.3℃). The model shows significant BC-induced warming over the central Eurasian region (>2℃) in JJA.

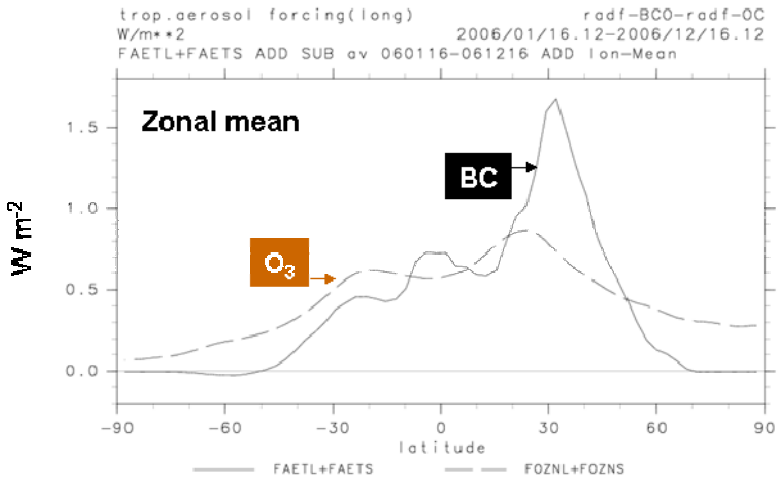

Fig. 5. Zonal averaged radiative forcing from tropospheric ozone increase and BC.

Major Publications

1) Yan, X. et al., Bottom-up estimates of biomass burning in mainland China, Atmos. Environ., 40, 5262-5273, 2006

2) Akimoto, H. et al., Verification of energy consumption in China during 1996-2003 by using satellite observational data, Atmos. Environ., 40, 7663-7667, 2006.

3) Yamaji, K., T. Ohara, I. Uno, H. Tanimoto, J. Kurokawa, and H. Akimoto, Analysis of seasonal variation of ozone in the boundary layer in East Asia using the Community Multi-scale Air Quality model: What controls surface Ozone level over Japan?, Atmos. Env., 40(10), 1856-1868, 2006..

4) Uno, I., Y. He, T. Ohara, K. Yamaji, J. Kurokawa, M. Katayama, Z. Wang, K. Noguchi, S. Hayashida, A. Richter, and J. P. Burrows, Systematic analysis of interannual and seasonal variations of model-simulated tropospheric NO_2 in Asia and comparison with GOME-satellite data, Atmos. Chem. Phys., 7, 1671-1681, 2006.

5) Tanimoto, H., H. Mukai, Y. Sawa, H. Matsueda, S. Yonemura, T. Wang, S. Poon, A. Wong, G. Lee, J.Y. Jung, K.R. Kim, M.H. Lee, N.H. Lin, J.L. Wang, C.F. Ou-Yang, C.F. Wu, H. Akimoto, P. Pochanart, K. Tsuboi, H. Doi, C. Zellweger, J. Klausen, Direct assessment of international consistency of standards for ground-level ozone: Strategy and implementation toward metrological traceability network in Asia, J. Environ. Monit., doi:10.1039/b701230f, 9, 1183-1193, 2007.

6) Wagner, T., et al., Comparison of Box-Air-Mass-Factors and Radiances for Multiple-Axis Differential Optical Absorption Spectroscopy (MAX-DOAS) Geometries calculated from different UV/visible Radiative Transfer Models, Atmos. Chem. Phys., 7, 1809-1833, 2007.

7) Noguchi, K., et al., Validation and comparison of tropospheric column ozone derived from GOME measurements with ozonesondes over Japan, SOLA, 3, 041-044, doi:10.2151/sola.2007-011, 2007.

8) Uno, I., et al., Systematic analysis of interannual and seasonal variations of model-simulated tropospheric NO_2 in Asia and comparison with GOME-satellite data, Atmos. Chem. Phys., 7, 1671-1681, 2007.

9) Ohara, T. et al., An Asian emission inventory of anthropogenic emission sources for the period 1980–2020, *Atmos. Chem. Phys.*, **7**, 4419-4444, 2007.

10) Uno, I., T. Ohara, K. Yamaji, and J. Kurokawa, Recent Trends and Future Projections in Asian Air Pollution, Journal of Disaster Research, 2(3), 163-172, 2007.

11) Sudo, K., and H. Akimoto, Global source attribution of tropospheric ozone: Long-range transport from various source regions, J. Geophys. Res., 112, D12302, doi:10.1029/2006JD007992, 2007.

12) Inomata, S., H. Tanimoto, S. Kameyama, U. Tsunogai, H. Irie, Y. Kanaya, and Z. Wang, Technical Note: Determination of formaldehyde mixing ratios in polluted air with PTR-MS: Laboratory experiments and field measurements, Atmos. Chem. Phys. 8, 273-284, 2008.

13) Irie, H., Y. Kanaya, H. Akimoto, H. Tanimoto, Z. Wang, J.F. Gleason, and E.J. Bucsela, Validation of OMI tropospheric NO_2 column data using MAX-DOAS measurements deep inside the North China Plain in June 2006, Atmos. Chem. Phys. Discuss., 8, 8243-8271, 2008.

14) Taketani, F., Y. Kanaya, and H. Akimoto, Kinetics of Heterogeneous Reactions of HO2 Radical at Ambient Concentration Levels with $(NH_4)_2SO_4$ and NaCl Aerosol Particles, J. Phys. Chem. A., 112/11 2370-2377, 2008.

15) Inomata, S., et al., Technical note: Determination of formaldehyde mixing ratios in polluted air with PTR-MS: laboratory experiments and field measurements, Atmos. Chem. Phys., 8, 273-284, 2008.

16) Irie, H., et al., First retrieval of tropospheric aerosol profiles using MAX-DOAS and comparison with lidar and sky radiometer measurements, Atmos. Chem. Phy., 8, 341-350, 2008.

17) Irie, H., et al., Validation of OMI tropospheric NO_2 column data using MAX-DOAS measurements deep inside the North China Plain in June 2006, Atmos. Chem. Phy. Discuss., 8, 8243-8271, 2008.

18) Yamaji, K., T. Ohara, I. Uno, J. Kurokawa, P. Pochanart, and H. Akimoto, 2008, Future Prediction of Surface Ozone over East Asia using Models-3 Community Multiscale Air Quality Modeling System (CMAQ) and Regional Emission Inventory in ASia (REAS), J. Geophys. Res., 113, D08306, doi:10.1029/2007JD008663, 2008.